Testing the Color Charge and Mass Dependence of Parton Energy Loss with Heavy-to-light Ratios at RHIC and LHC

Néstor Armesto[1,2], Andrea Dainese[3], Carlos A. Salgado[1] and Urs Achim Wiedemann[1]

[1] *Department of Physics, CERN, Theory Division, CH-1211 Genève 23, Switzerland*

[2] *Departamento de Física de Partículas and Instituto Galego de Altas Enerxías, Facultade de Física, Campus Sur, Universidade de Santiago de Compostela, 15782 Santiago de Compostela, Spain*

[3] *Università degli Studi di Padova and INFN, via Marzolo 8, 35131 Padova, Italy*

February 11, 2014

The ratio of nuclear modification factors of high-p_T heavy-flavored mesons to light-flavored hadrons ("heavy-to-light ratio") in nucleus-nucleus collisions tests the partonic mechanism expected to underlie jet quenching. Heavy-to-light ratios are mainly sensitive to the mass and color-charge dependences of medium-induced parton energy loss. Here, we assess the potential for identifying these two effects in D and B meson production at RHIC and at the LHC. To this end, we supplement the perturbative QCD factorized formalism for leading hadron production with radiative parton energy loss. For D meson spectra at high but experimentally accessible transverse momentum ($10 \lesssim p_T \lesssim 20$ GeV) in Pb–Pb collisions at the LHC, we find that charm quarks behave essentially like light quarks. However, since light-flavored hadron yields are dominated by gluon parents, the heavy-to-light ratio of D mesons is a sensitive probe of the color charge dependence of parton energy loss. In contrast, due to the larger b quark mass, the medium modification of B mesons in the same kinematical regime provides a sensitive test of the mass dependence of parton energy loss. At RHIC energies, the strategies for identifying and disentangling the color charge and mass dependence of parton energy loss are more involved because of the smaller kinematical range accessible. We argue that at RHIC, the kinematical regime best suited for such an analysis of D mesons is $7 \lesssim p_T \lesssim 12$ GeV, whereas the study of lower transverse momenta is further complicated due to the known dominant contribution of additional, particle species dependent, non-perturbative effects.

1. Introduction

High-p_T partons, produced in dense QCD matter, are expected [1–6] to suffer a significant additional medium-induced energy degradation prior to hadronization in the vacuum. Models based on this picture [7–13] account for the main modifications of high-p_T hadron production in nucleus-nucleus collisions at RHIC, namely the strong suppression of single inclusive hadron spectra, their centrality dependence [14–19], the corresponding suppression of leading back-to-back correlations [20], and high-p_T hadron production with respect to the reaction plane [21]. To further test the microscopic dynamics of medium-induced parton energy loss, two classes of measurements are now gradually coming into experimental reach [22]: First, high-p_T particle correlations [23–25], jet shapes and jet multiplicity distributions [26–29] will test the predicted relation between the energy loss of the leading parton, the transverse momentum broadening of the parton shower, and the softening of its multiplicity distribution. Second, the relative yields of identified high-p_T hadrons will test the prediction that medium-induced parton energy loss depends on the identity of the parent parton. Hard gluons lose more energy than hard quarks due to the stronger coupling to the medium [1–6], and the energy loss of massive quarks is further reduced [30–33] due to the mass-dependent restriction of the phase space into which medium-induced gluon radiation can take place.

In the present work, we calculate the nuclear modification factor for single inclusive high-p_T spectra of charmed and beauty mesons, supplementing the perturbative QCD factorized formalism with radiative parton energy loss. We also calculate the ratio of nuclear modification factors of heavy-flavored mesons to light-flavored hadrons ("heavy-to-light ratios"). In general, heavy-to-light ratios are sensitive to the following medium-induced effects:

1. *Color charge dependence of parton energy loss:*
   In contrast to charmed and beauty mesons, light-flavored hadron spectra receive a significant p_T dependent contribution from hard fragmenting gluons. Gluons are expected to lose more energy due to their stronger coupling to the medium. This increases heavy-to-light ratios at all p_T.
2. *Mass dependence of parton energy loss:*
   Massive quarks are expected to lose less energy in a medium than light quarks. This further enhances heavy-to-light ratios as long as the parton mass is not negligible compared to the partonic p_T.
3. *Medium-dependent trigger bias due to p_T spectrum of parent parton:*
   Up to rather high transverse momentum, the partonic p_T spectrum of massive quarks is less steep than that of light quarks. For a more steeply falling spectrum, the same parton energy loss leads to a stronger reduction of the nuclear modification factor [9, 34]. This enhances heavy-to-light

ratios.

4. *Medium-dependent trigger bias due to fragmentation of parent parton:* Heavy quark fragmentation functions are significantly harder than light quark ones. The same parton energy loss leads to a stronger reduction of the nuclear modification factor if the fragmentation function is harder [35]. This reduces heavy-to-light ratios.

Our aim is to establish —for the kinematical ranges accessible at RHIC and at the LHC— the relative importance of these contributions to heavy-to-light ratios. In this way, we want to assess the potential of such measurements for further clarifying the partonic mechanism conjectured to underlie jet quenching in nucleus-nucleus collisions. The theoretical framework of our study is introduced in Section 2, and results for the nuclear modification of heavy quark spectra at RHIC and at the LHC are given in Sections 3 and 4, respectively. We then summarize our main conclusions.

2. The formalism

The nuclear modification factor $R_{AB}(p_T)$ determines the modification of the production of a hadron h in a nucleus-nucleus collisions A–B compared to an equivalent number of proton-proton collisions,

$$R_{AB}(p_T) = \frac{\left.\frac{\mathrm{d}N^{AB\to h}_{\mathrm{medium}}}{\mathrm{d}p_T\,\mathrm{d}y}\right|_{y=0}}{\langle N^{AB}_{\mathrm{coll}}\rangle \left.\frac{\mathrm{d}N^{pp\to h}_{\mathrm{vacuum}}}{\mathrm{d}p_T\,\mathrm{d}y}\right|_{y=0}} \,. \tag{2.1}$$

Here, $\langle N^{AB}_{\mathrm{coll}}\rangle$ is the average number of inelastic nucleon–nucleon collisions in a given centrality class. It is proportional to the average nuclear overlap function $\langle T_{AB}\rangle$, which is defined via the convolution of the nuclear thickness functions $T_{A,B}(\mathbf{s})$ as an integral over the transverse plane at fixed impact parameter $\mathbf{b}$, $T_{AB}(b) = \int \mathrm{d}\mathbf{s}\, T_A(\mathbf{s})\, T_B(\mathbf{b}-\mathbf{s})$.

To calculate the yield of the hadron species h from a parent parton $k = q, Q, g$ (a massless or massive quark or a gluon) produced at rapidity $y = 0$ with transverse momentum p_T, we start from a collinearly factorized expression supplemented by parton energy loss [8, 9],

$$\left.\frac{\mathrm{d}N^{AB\to h}_{\mathrm{medium}}}{\mathrm{d}p_T\,\mathrm{d}y}\right|_{y=0} = \sum_{i,j}\int \mathrm{d}x_i\,\mathrm{d}x_j\,\mathrm{d}(\Delta E/E)\,\mathrm{d}z_k\, f_{i/A}(x_i)\, f_{j/B}(x_j) \times \left.\frac{\mathrm{d}\hat{N}^{ij\to k}(p_{T,k}+\Delta E)}{\mathrm{d}p_{T,k}\mathrm{d}y}\right|_{y=0} P(\Delta E/E, R, \omega_c, m/E)\,\frac{D_{k\to h}(z_k)}{z_k^2}\,. \tag{2.2}$$

Here, $f_{i/A}(x_i)$ and $f_{j/B}(x_j)$ denote the nuclear parton distribution functions for partons i, j carrying momentum fractions x_i, x_j in the colliding nuclei A, B, respectively. The total energy of the produced parton is denoted by E, its medium-induced parton energy loss by ΔE. The produced hadron carries a fraction $z = p_T/p_{T,k}$ of the transverse momentum $p_{T,k}$ of the parent parton. The hard partonic scattering cross section for the production $i + j \to k + X$ reads $\mathrm{d}\hat{N}^{ij\to k}(p_{T,k} + \Delta E)/\mathrm{d}p_{T,k}\mathrm{d}y$. The fragmentation function $D_{k\to h}(z_k)$ maps the parton k onto the hadron h. We work at $y = 0$ where the parton energy is comparable to the parton transverse momentum, $E \simeq p_{T,k}$. This sets the factorization and renormalization scales which are implicitly present in (2.2).

The final state medium-dependence enters (2.2) via the probability $P(\epsilon, R, \omega_c, m/E)$ that the parton loses an additional energy fraction $\epsilon = \Delta E/E$ due to medium-induced gluon radiation prior to hadronization in the vacuum. This so-called quenching weight depends on the in-medium path length of the hard parton and on the density of the medium, parametrized by the variables R and ω_c. For charm and beauty quarks, it also depends on the quark mass. Details of the definition of the model parameters and of the calculation of P are given in Appendix A and Section 2 B below.

A. Benchmark results without parton energy loss

To establish the baseline for the nuclear modification factor (2.1), we calculate first the high-p_T particle yields (2.2) for identified light and heavy-flavored hadrons in the absence of final state medium effects. Without medium, the quenching weight takes the form

$$P(\Delta E/E, R, \omega_c, m/E) = \delta(\Delta E/E)\,, \qquad \text{(vacuum)}, \tag{2.3}$$

and Eq. (2.2) reduces to the standard collinearly factorized leading order perturbative QCD formalism. For this baseline, we rely on the PYTHIA event generator (version 6.214) [36], paralleling the approach used in Ref. [8] for light-flavored hadrons. As input, we use CTEQ 4L parton distribution functions [37] with EKS98 nuclear corrections [38]. All partonic subprocesses $gg \to Q\overline{Q}$, $q\overline{q} \to Q\overline{Q}$, $Qg \to Qg$, $\overline{Q}g \to \overline{Q}g$ and gluon splitting $g \to Q\overline{Q}$ are included in PYTHIA (option MSEL = 1). PYTHIA also accounts for the possibility that a $Q\overline{Q}$-pair is created by (vacuum) gluon radiation from the primary partons created in the hard collision. This effect becomes significant at the LHC but is negligible at RHIC. The splitting $g \to Q\overline{Q}$ requires a high virtuality gluon ($\gtrsim 2\,m_Q$) which corresponds to a short formation time. Hence, we shall assume later that heavy quark pairs from such a secondary $g \to Q\overline{Q}$ production process have the same in-medium path length as those produced directly in

the hard scattering process.

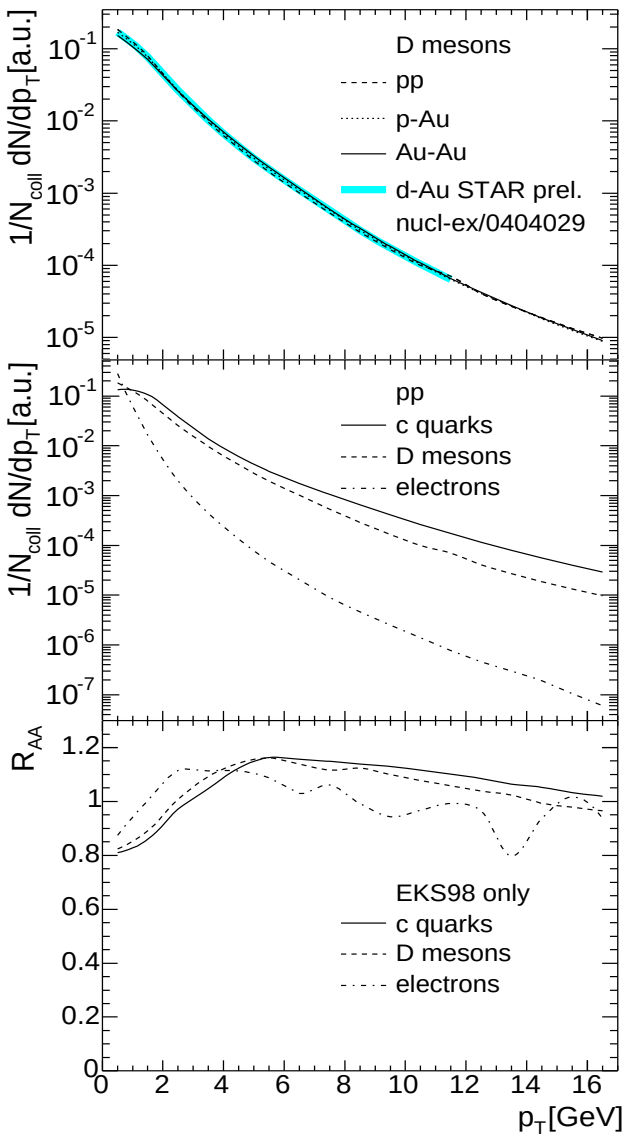

Fig. 1. Upper and central panels: transverse momentum spectra for D mesons, c quarks and electrons from charm decays in pp, p–Au and Au–Au collisions at $\sqrt{s_{NN}} = 200$ GeV. The shaded band in the upper panel corresponds to a parameterization of data from the STAR Collaboration [39,40]. Lower panel: nuclear modification factor for c quarks, D mesons and electrons from charm decay in Au–Au collisions at $\sqrt{s_{NN}} = 200$ GeV. Except for the nuclear modification of parton distribution functions according to EKS98 [38], no medium effects have been included.

Our parameterization of the fragmentation functions in (2.2) is based on the string model implemented in PYTHIA. In particular, we generate with PYTHIA pp events which contain charm (or beauty) quarks and we force the semi-electronic decay of corresponding heavy-flavored mesons. From these

events we extract the heavy quark yields and the probabilities for a quark k of transverse momentum $p_{T,k}$ to fragment into a hadron h with p_T [and further into an electron with $p_{T,e}$]. These probabilities will be used as fragmentation functions.

For RHIC energy, $\sqrt{s_{NN}} = 200$ GeV, charm production in PYTHIA was tuned to reproduce, in shape, the experimental data on the D meson p_T distribution in d–Au collisions measured by the STAR Collaboration [39,40]. This baseline for charm production at RHIC is presented in Fig. 1. The p_T distribution of D mesons traces closely that of their parent c quarks, but the distribution of electrons is considerably softer. This complicates attempts to study heavy quark parton energy loss on the basis of single inclusive electron spectra [41, 42]. Nuclear modifications of the parton distribution functions are seen to affect the p_T spectra at most by $\pm 20\%$ at low p_T.

For LHC energy, $\sqrt{s_{NN}} = 5.5$ TeV, we use a tuning of PYTHIA [43] that reproduces the shape of the p_T distributions for charm and beauty quarks given by pQCD calculations at next-to-leading order [44] with CTEQ 4M parton distribution functions, $m_c = 1.2$ GeV and factorization and renormalization scales $\mu_F = \mu_R = 2\, m_T$ for charm, and $m_b = 4.75$ GeV and $\mu_F = \mu_R = m_T$ for beauty, where $m_T^2 = m_Q^2 + p_T^2$.

B. Modeling the medium dependence of parton energy loss

Medium-induced parton energy loss depends on the in-medium path length and the density of the medium. It is characterized by the medium-induced gluon energy distribution $\omega dI^{\rm med}/d\omega$ radiated off the hard parton. This defines the probability distribution for medium-induced energy loss ("quenching weight P"), entering the cross section (2.2) for medium-modified high-p_T hadron production. Further details of this procedure are given in Appendix A.

The dependence of parton energy loss on density and in-medium path length can be characterized in terms of the time-dependent BDMPS transport coefficient $\hat{q}(\xi)$ which denotes the average squared transverse momentum transferred from the medium to the hard parton per unit path length. Numerically, one finds that the effects of a time-dependent density of the medium on parton energy loss can be accounted for by an equivalent static medium, specified in terms of the time-averaged model parameters ω_c and R,

$$\omega_c \equiv \int_0^\infty {\rm d}\xi\, \xi\, \hat{q}(\xi)\,, \tag{2.4}$$

$$R = \frac{2\omega_c^2}{\int_0^\infty {\rm d}\xi\, \hat{q}(\xi)}\,. \tag{2.5}$$

For light quarks and gluons, the quenching weights $P(\Delta E/E, R, \omega_c)$ have been calculated in Ref. [45] and they are available as a CPU-inexpensive FORTRAN routine. For the purpose of this work, we have extended this calculation to the case of quenching weights $P(\Delta E/E, R, \omega_c, m/E)$ for massive quarks, starting from the medium-induced gluon energy distribution determined in Ref. [31]. Results for these quenching weights are given in Appendix A and they are publicly available as a CPU-inexpensive FORTRAN routine accompanying this paper [46].

We sample the positions $\mathbf{s} = (x_0, y_0)$ of the parton production points in the transverse plane of a nucleus-nucleus collision A–B with the probability given by the product of the nuclear thickness functions $T_A(\mathbf{s})\, T_B(\mathbf{b} - \mathbf{s})$. For these thickness functions, we choose Woods-Saxon parameterizations of nuclear density profiles [47]. For a hard parton with production point $\mathbf{s} = (x_0, y_0)$ and azimuthal propagation direction $\mathbf{n} = (n_x, n_y)$, the local transport coefficient along the path of the parton is defined as [8]:

$$\hat{q}(\xi) = k\, T_A(\mathbf{s} + \xi\mathbf{n})\, T_B(\mathbf{b} - [\mathbf{s} + \xi\mathbf{n}])\,. \tag{2.6}$$

Here, the constant k sets the scale of the transport coefficient. This defines ω_c and R in (2.4) and (2.5). All values of transport coefficients used in this work characterize time-averaged properties of the medium —their numerical value is determined by the established relation [45] between parton energy loss in a dynamically expanding and a static medium.

Partons that lose their entire energy due to medium effects are redistributed in our formalism according to a thermal distribution [48],

$$\left.\frac{\mathrm{d}N_{\mathrm{thermal}}}{\mathrm{d}m_T\,\mathrm{d}y}\right|_{y=0} \propto m_T\, \exp\left(-\frac{m_T}{T}\right). \tag{2.7}$$

For the following results, we use $T = 300$ MeV. By varying T between 5 and 500 MeV, we have checked that the choice of T affects the nuclear modification factor (2.1) only for $p_T \lesssim 3$ GeV. The reasons why the present parton energy loss formalism is not reliable at such low transverse momenta have been mentioned repeatedly [22, 45]. Accordingly, the main conclusions drawn from our study will be for significantly higher transverse momentum.

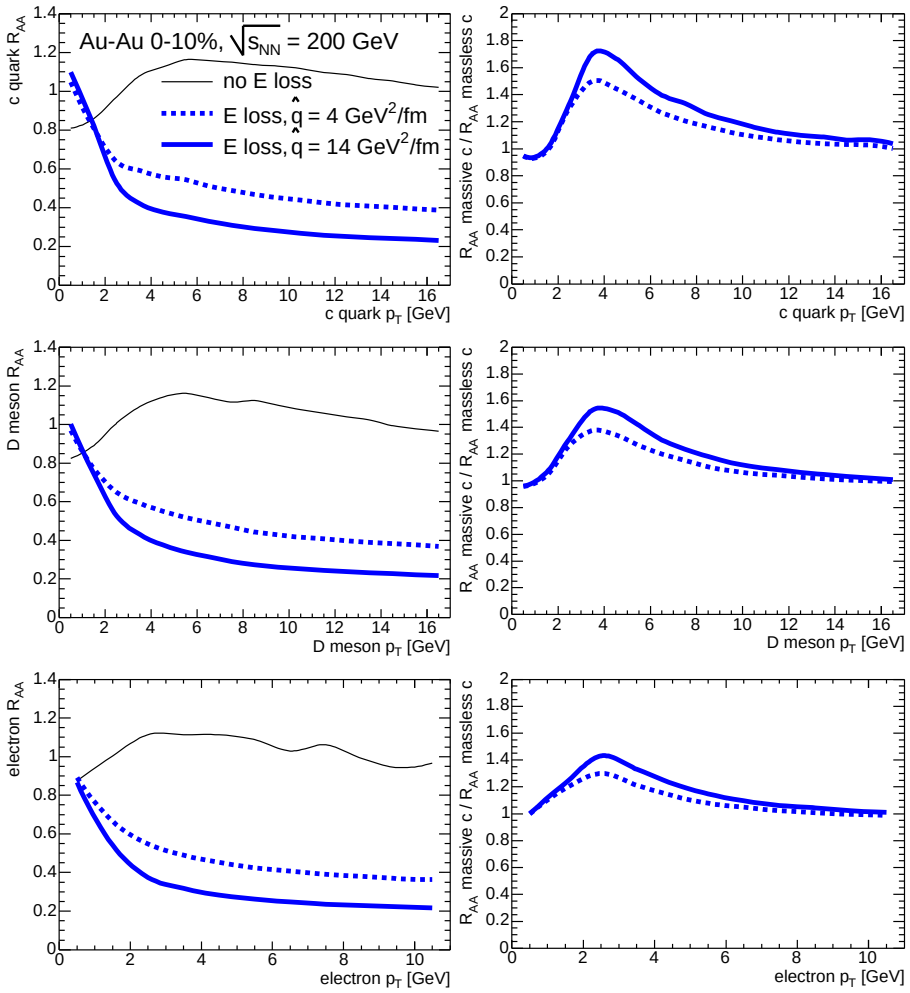

Fig. 2. LHS: Nuclear modification factors for c quarks, D mesons and their decay electrons in central (0–10%) Au–Au collisions at $\sqrt{s_{NN}} = 200$ GeV for different time-averaged strengths of the parton energy loss. RHS: The ratio of the nuclear modification factor plotted on the LHS, divided by the same factor calculated for a massless charm quark.

3. Results for RHIC

Recent model studies of the nuclear modification of light-flavored hadrons in Au–Au collisions at RHIC favor a time-averaged transport coefficient $\hat{q} \approx 4 \div 14$ GeV^2/fm [8, 9]. To account for the significant systematic uncertainties of this favored value, we calculate here the particle yield (2.2) for $\hat{q} = 0$, 4 and 14 GeV^2/fm. The corresponding nuclear modification factors are shown in Fig. 2 for D mesons, c quarks and for electrons from charm decay. To illustrate the mass dependence of parton energy loss, we compare the calculation for a realistic charm quark mass $m_c = 1.2$ GeV to the hypothetical case that the

charm quark loses as much energy as a light quark. The ratio of the two nuclear modification factors thus obtained is shown in Fig. 2. One sees that the mass dependence of final state parton energy loss leads to a significant change of the nuclear modification factor of D mesons up to transverse momenta of $p_T \lesssim 12$ GeV. This is consistent with the general observation that the mass dependence of parton energy loss is a function of m/E and becomes negligible for $m/E < 0.1$ [31].

In Fig. 2, one also sees that the ratio of the realistic nuclear modification factor to the one for $m_c = 0$ GeV has a maximum around $p_T \sim 2$–4 GeV, and drops slightly below unity for very small p_T. This is a generic consequence of the fact that parton energy loss redistributes charm quarks towards the softer region in transverse phase space. If the depletion at high p_T is less significant due to a finite parton mass, then the resulting enhancement at small p_T is also less significant and this depletes the ratio of nuclear modification factors. However, at smaller transverse momentum, $p_T < 7$ GeV, soft hadron production or non-perturbative hadronization mechanisms in the medium like recombination or coalescence [49–51] (and the possibility of thermalization [52,53] and collisional energy loss [54,55]) have to be considered [22] to account for the sizable particle species dependence of the nuclear modification factors [56, 57]. Here, parton energy loss alone cannot be expected to provide a reliable description. This complicates the analysis of heavy meson spectra and their decay products at low p_T [58]. As a consequence, the following discussion will mainly focus on the region $p_T > 7$ GeV.

As explained in the Introduction, the mass dependence of parton energy loss displayed in Fig. 2 is only one of several parton species dependent modifications of parton energy loss. Other modifications result from the dependence of parton energy loss on the color charge of the parent parton, and from trigger bias effects related to the partonic p_T spectrum and the parton fragmentation function. To disentangle the relative strength of these effects, we plot in Fig. 3 the heavy-to-light ratio $R_{D/h} = R^D_{AA}/R^h_{AA}$ (h referring to light-flavored hadrons) for model calculations in which the above mentioned mass-sensitive medium dependences have been switched off selectively.

Parametrically, the mass dependence of the medium-induced parton energy loss and of the trigger biases becomes negligible at high transverse momentum where $m_c/p_T \to 0$. In contrast, the difference between quark and gluon energy loss stays at all p_T due to the ratio of the Casimir factors $C_A/C_F = 9/4$. Hence, at the highest p_T, the color charge dependence of parton energy loss dominates the difference between the nuclear modification factor for light-flavored and heavy-flavored hadrons. In agreement with this argument, Fig. 3 shows that the color charge dependence accounts for the dominant deviation of $R_{D/h}$ from unity for $p_T \gtrsim 12$ GeV. At such high transverse momentum, charm quarks start to behave like light quarks and the heavy-to-light ratio of

D mesons becomes mainly sensitive to the color charge dependence of parton energy loss. However, at RHIC energies, the corresponding signal is rather small, see Fig. 3. In combination with the small high-p_T cross sections, this may limit a quantitative study of this interesting kinematical regime.

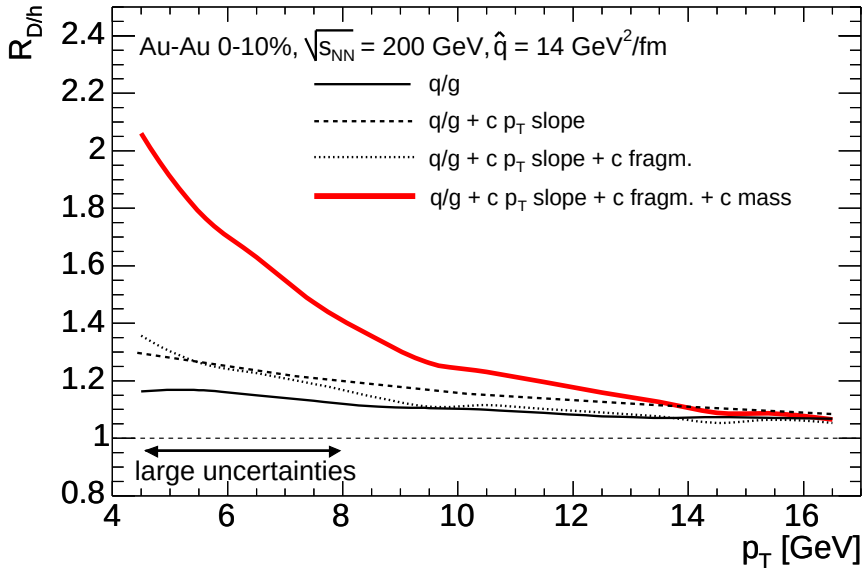

Fig. 3. Different contributions to the heavy-to-light ratio of D mesons in central (0–10%) Au–Au collisions at $\sqrt{s_{NN}} = 200$ GeV. Different curves correspond to the case in which the charm distribution is described i) with the same p_T spectrum, fragmentation function and parton energy loss as a light quark, ii) with a realistic charm p_T spectrum only, iii) with the charm p_T spectrum and fragmentation function of a realistic charm quark and iv) for the realistic case which includes the mass dependence of parton energy loss.

Medium-dependent trigger bias effects due to the mass dependence of the partonic p_T spectrum and due to the fragmentation function largely compensate each other. They go in the directions indicated by the general arguments in the Introduction, but they are negligible over the entire p_T range displayed in Fig. 3.

The mass dependence of parton energy loss dominates the deviation of $R_{D/h}$ from unity for $p_T < 12$ GeV. However, as discussed above, the particle species dependence of R_{AA} for $p_T \lesssim 7$ GeV [56, 57] makes the application of parton energy loss questionable. Thus, to assess the mass dependence of parton energy loss with the heavy-to-light ratio $R_{D/h}$ at RHIC, one should focus on the kinematical region, $7 \lesssim p_T \lesssim 12$ GeV. Even in that region, the color charge effect is sizable and has to be taken into account in a quantitative analysis, see Fig. 3.

4. Results for the LHC

To calculate the nuclear modification of high-p_T particle yields in Pb–Pb collisions at LHC energy $\sqrt{s_{NN}} = 5500$ GeV, the density of the produced matter has to be characterized, e.g. by the BDMPS transport coefficient $\hat{q}$, see Section 2. This transport coefficient is proportional to the particle multiplicity in the collision. In Refs. [8, 9] the relative increase of the event multiplicity from RHIC to LHC has been taken to be ~ 7 [59], but other more recent estimates give a significantly smaller increase ~ 2.6 [60]. Here, we scan a very wide range of the model parameter space by varying $\hat{q}$ between a low estimate at RHIC energies and the highest estimates for LHC energies, $\hat{q} = 4$, 25 and 100 GeV^2/fm.

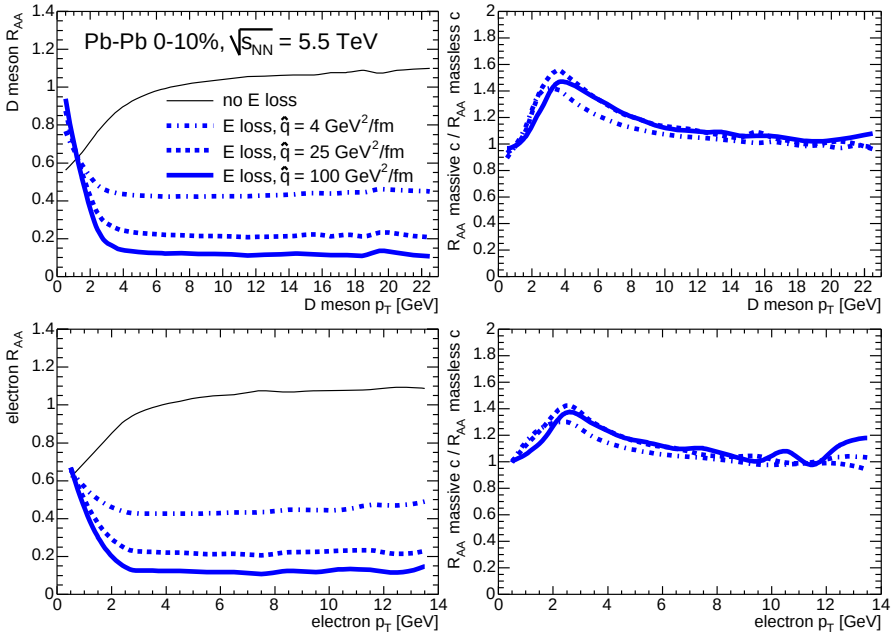

Fig. 4. LHS: Nuclear modification factors for D mesons (upper plot) and electrons from charm decays (lower plot) in central (0–10%) Pb–Pb collisions at $\sqrt{s_{NN}} = 5.5$ TeV. RHS: The ratio of the realistic nuclear modification factors shown on the left hand side and the same factors calculated by solely neglecting the mass dependence of parton energy loss.

At the LHC as at RHIC, a significant mass dependence of the nuclear modification factor of D mesons and of their decay electrons is limited to transverse momenta below $p_T \lesssim 10$ GeV, see Fig. 4. However, at the LHC, there are arguments that non-perturbative hadronization mechanisms such as recombination may dominate the medium modification of identified particle yields up to even higher transverse momenta than at RHIC [61]. Thus, the mass dependence of parton energy loss will dominate the deviation of the heavy-to-light

ratio of D mesons from unity only in a rather small kinematical window, if at all.

At higher transverse momenta, $p_T \gtrsim 10$ GeV, the charm mass dependence of parton energy loss becomes negligible since $m_c/p_T \to 0$, see Fig. 4. Remarkably, however, even if charm mass effects are neglected, the heavy-to-light ratio $R_{D/h}$ shows for realistic model parameters a significant enhancement $R_{D/h} \sim 1.5$ in a theoretically rather clean and experimentally accessible kinematical regime of high transverse momenta $10 \lesssim p_T \lesssim 20$ GeV, see Fig. 5 (upper panels). The reason is that parton production at mid-rapidity tests values of Bjorken x which are a factor ~ 30 smaller at LHC than at RHIC. At smaller Bjorken x, a larger fraction of the produced light-flavored hadrons have gluon parents and thus the color charge dependence of parton energy loss can leave a much more sizable effect in the heavy-to-light ratio $R_{D/h}$ at LHC. In summary, charm quarks giving rise to D mesons in the kinematical range $10 \lesssim p_T \lesssim 20$ GeV behave essentially like massless quarks in Pb–Pb collisions at the LHC. But the significant gluonic contribution to light-flavored hadron spectra in this kinematical range makes the heavy-to-light ratio $R_{D/h}$ a very sensitive hard probe for testing the color charge dependence of parton energy loss.

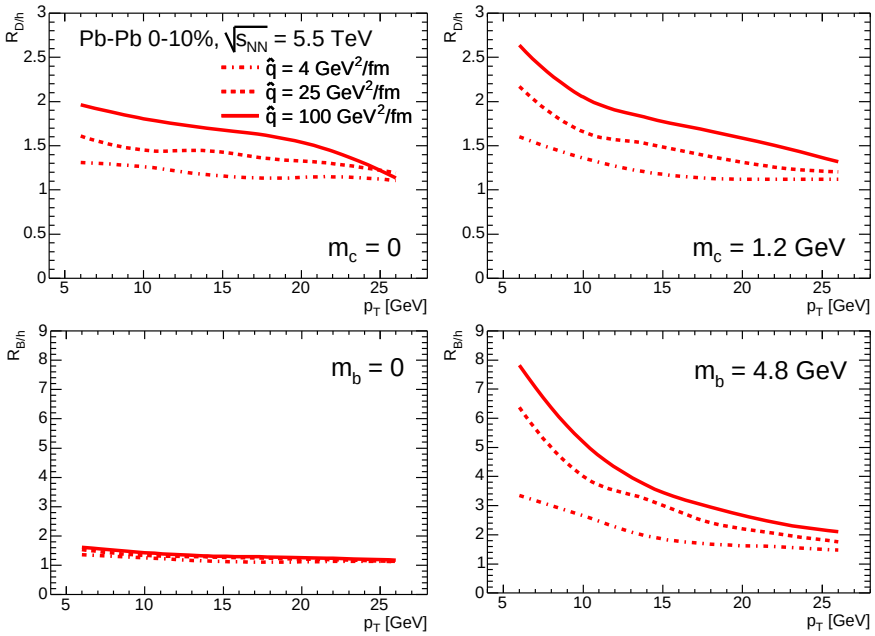

Fig. 5. Heavy-to-light ratios for D mesons (upper plots) and B mesons (lower plots) for the case of a realistic heavy quark mass (plots on the right) and for a case study in which the quark mass dependence of parton energy loss is neglected (plots on the left).

At the higher LHC energies, the higher mass scale of b quarks can be tested

in the corresponding nuclear modification factors and heavy-to-light ratios for B mesons and for electrons from b decays. As seen in Figs. 5 and 6, for transverse momenta $10 \lesssim p_T \lesssim 20$ GeV, the mass dependence of parton energy loss modifies the nuclear modification factor by a factor 2 or more. It dominates over the color charge dependence. As for all spectra discussed above, the medium-dependence of trigger bias effects is rather small for beauty production at the LHC [In Fig. 5, these trigger bias effects account for the small but visible differences between $R_{D/h}$ and $R_{B/h}$ in the model calculation in which the mass dependence of parton energy loss has been neglected.]. We conclude that the heavy-to-light ratio $R_{B/h}$ in Pb–Pb collisions at the LHC provides a very sensitive hard probe for testing the parton mass dependence of parton energy loss in the theoretically rather clean and experimentally accessible kinematical regime of $10 \lesssim p_T \lesssim 20$ GeV.

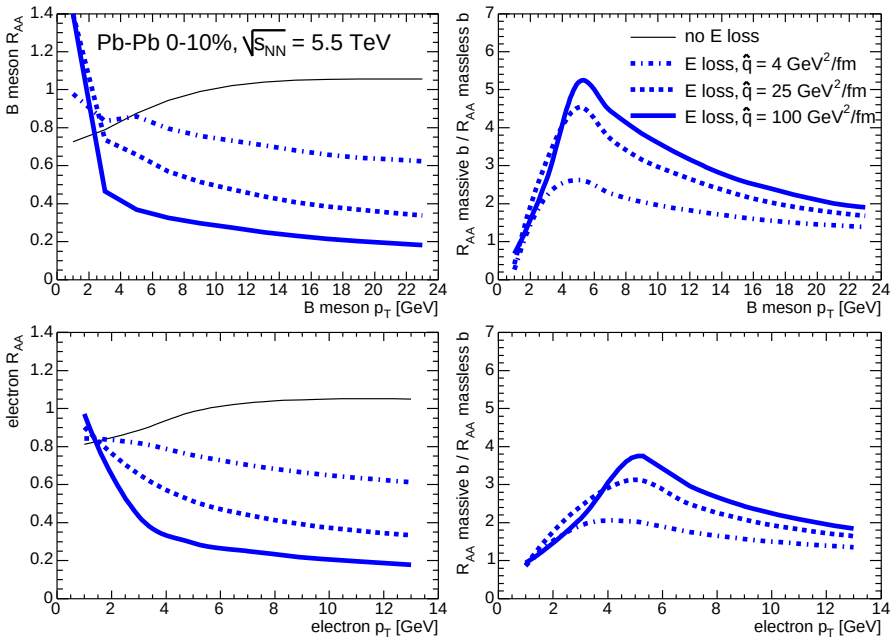

Fig. 6. The same as Fig. 4 but for B mesons and electrons from beauty decays.

5. Conclusions

The mass dependence of parton energy loss and its phenomenological consequences for heavy-to-light ratios have received significant interest recently [30–33, 62–66], since they provide a tool to test the conjectured microscopic dynamics underlying the phenomenon of high-p_T hadron suppression at RHIC. Here, we have shown that heavy-to-light ratios are not solely sensitive to the mass dependence of parton energy loss, but also to its color charge dependence. The task for both experiment and theory is to identify and to disentangle both

effects. This issue is of fundamental importance since the more precise understanding of the dynamics modifying a hard probe is a prerequisite for the more precise understanding of the properties of what is probed, namely dense QCD matter.

Previous proposals to search for the color charge dependence of parton energy loss either tried to exploit the weak p_T dependence of the quark-to-gluon ratio of parent partons in light-flavored hadron spectra [67]. Alternatively, they focused on proton-to-antiproton ratios at high p_T [68]. Since antibaryons receive a larger fragmentation contribution from gluon parents, parton energy loss predicts an increase of the $p/\overline{p}$ ratio with increasing p_T. However, the kinematical range for studying proton-to-antiproton ratios is rather restricted due to experimental limitations on measuring identified baryons at high-p_T, and due to the anomalous baryon-to-meson ratio which complicates the physics interpretation at intermediate p_T ($p_T \lesssim 7$ GeV). Similar caveats apply to the ratio $\Lambda/\overline{\Lambda}$. This baryon-to-antibaryon ratio may have the experimental advantage that it can be measured via topological reconstruction to higher p_T than the $p/\overline{p}$ ratio. However, its sensitivity to the medium-modification of parton dynamics remains to be assessed, and may be complicated due to our limited knowledge about Λ fragmentation functions. Compared to these measurements, the heavy-to-light ratios of D mesons have significant experimental and theoretical advantages. In particular, in Pb–Pb collisions at the LHC, they show a high sensitivity to the color charge dependence of parton energy loss in a kinematical range $10 \lesssim p_T \lesssim 20$ GeV in which charm quarks behave like light quarks and other medium modifications are expected to be negligible, see Section 4. Thus, they provide a unique way to "tag" a light quark (namely the charm quark) since they can be characterized experimentally by cross-checking several relatively clean decay channels.

On the other hand, the heavy-to-light ratio of B mesons in the same kinematical regime $10 \lesssim p_T \lesssim 20$ GeV at the LHC is expected to be predominantly sensitive to the mass dependence of parton energy loss, showing significant enhancement factors of the order $2 \div 5$, see Section 4. Thus, a combined analysis of open charm and beauty mesons at the LHC provides the means to quantify and to disentangle the characteristic differences of the strength of the parton energy loss for the different identities of the parent parton.

In nucleus-nucleus collisions at RHIC, the task of identifying and disentangling the color charge and mass dependence of parton energy loss is more challenging, since a significantly smaller kinematical range of high transverse momentum is experimentally accessible. In particular, the region up to at least $p_T \lesssim 7$ GeV can only provide circumstantial evidence to this end, since it is known to receive significant additional particle species dependent nonperturbative contributions. In view of the present study, the first use of RHIC heavy meson spectra in the context of testing parton energy loss is to test the

combined effect of the mass and color charge dependence of parton energy loss in the kinematical range $7 \lesssim p_T \lesssim 12$ GeV where $R_{D/h}$ is expected to be gently but visibly enhanced above unity, see Section 3.

We finally note that correlation measurements may provide important complementary information for elucidating the influence of parton identity on final state parton energy loss. For example, requiring that a high-p_T trigger hadron at forward rapidity is balanced by a recoil at mid-rapidity, one may be able to study medium-modified hadron production in a configuration which enriches the contribution of gluon parents. Both at RHIC and at the LHC, the class of correlation measurements with this potential is large. It includes many as yet unexplored observables such as three jet events which in large acceptance experiments at the LHC may give access to the study of well-separated samples of quark and gluon jets. These correlations lie outside the scope of the present work. To the best of our knowledge, it is an open question whether some of them have a similar or even higher sensitivity to the mass and color charge dependence of parton energy loss than the ratios of particle identified single inclusive hadron spectra studied here.

Acknowledgment: We thank Peter Jacobs for helpful discussions.

A. Quenching weights for massive partons

In this appendix, we give details of how to calculate the probability $P(\Delta E/\omega_c, R, m/E)$ that a quark of mass m and initial energy E loses an energy fraction $\Delta E/E$ due to medium-induced gluon radiation.

We start from the medium-induced distribution of gluons of energy ω and transverse momentum $\mathbf{k}_\perp$, radiated off the hard massive quarks due to multiple scattering in the spatially extended medium [31]

$$\omega \frac{dI^{\rm med}}{d\omega\, d\mathbf{k}_\perp} = \frac{\alpha_s\, C_F}{(2\pi)^2\, \omega^2}\, 2{\rm Re} \int_0^\infty {\rm d}y_l \int_{y_l}^\infty {\rm d}\bar{y}_l\, e^{i\bar{q}(y_l-\bar{y}_l)} \int {\rm d}\mathbf{u}\, e^{-i\mathbf{k}_\perp\cdot\mathbf{u}}\, e^{-\frac{1}{2}\int_{\bar{y}_l}^\infty {\rm d}\xi\, n(\xi)\,\sigma(\mathbf{u})} \times \frac{\partial}{\partial \mathbf{y}}\cdot\frac{\partial}{\partial \mathbf{u}} \int_{\mathbf{y}=0=\mathbf{r}(y_l)}^{\mathbf{u}=\mathbf{r}(\bar{y}_l)} \mathcal{D}\mathbf{r} \exp\left[i\int_{y_l}^{\bar{y}_l} {\rm d}\xi \frac{\omega}{2}\left(\dot{\mathbf{r}}^2 - \frac{n(\xi)\sigma(\mathbf{r})}{i\,\omega}\right)\right]. \quad \text{(A.1)}$$

The strong coupling constant α_s and Casimir operator $C_F = \frac{4}{3}$ determine the coupling strength of gluons to the massive quark. The physical interpretation of the internal integration variables in (A.1) has been explained elsewhere [31,45] and plays no role in what follows. For numerical calculations, we use $\alpha_s = 1/3$. Eq. (A.1) resums the effects of arbitrary many medium-induced scatterings to leading order in $1/E$.

The parton mass dependence enters the gluon energy distribution (A.1) via the phase factor $\exp\left[i\bar{q}(y_l - \bar{y}_l)\right]$ [31], where $\bar{q}$ is defined as the difference between the total three momentum of the initial quark (p_1), and the final quark (p_2) and gluon (k),

$$\bar{q} = p_1 - p_2 - k \simeq \frac{x^2\, m^2}{2\omega}\,, \qquad x = \frac{\omega}{E}\,. \tag{A.2}$$

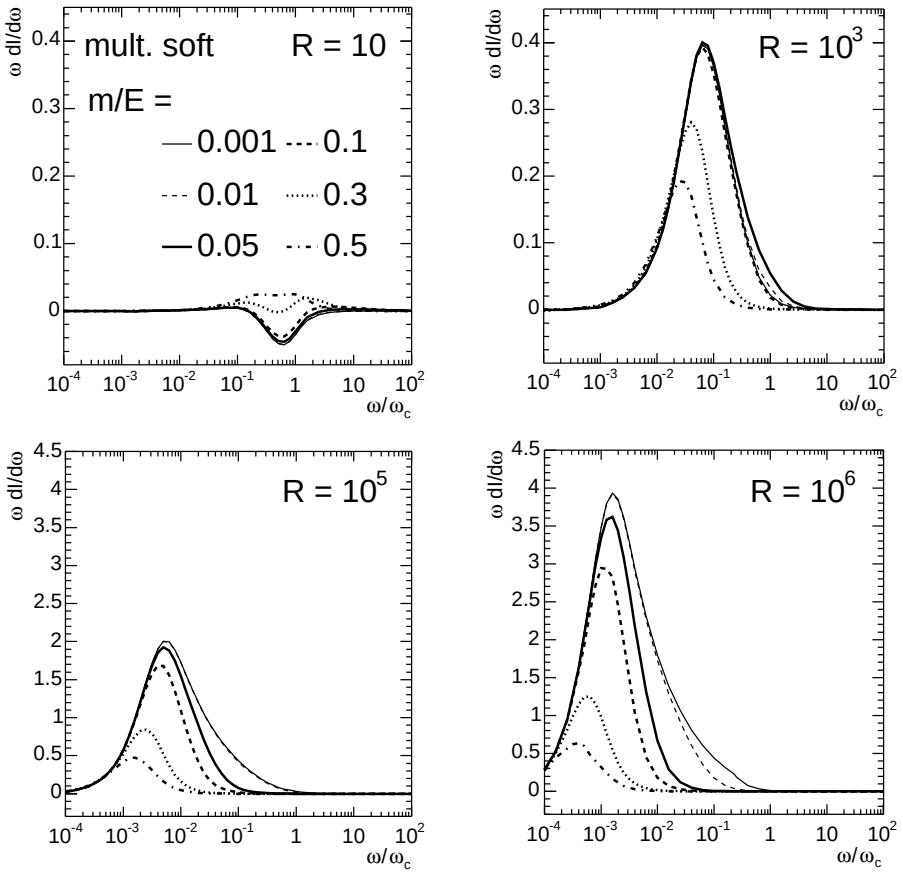

Fig. A.1. The k_T integrated medium-induced gluon energy distribution (A.1) radiated off a massive quark for different values of R (panels) and of m/E (line styles).

The medium-dependence enters (A.1) via the product of the time-dependent density $n(\xi)$ of scattering centers times the strength of a single elastic scattering $\sigma(\mathbf{r})$. In what follows, we work in the multiple soft scattering approximation

$$n(\xi)\sigma(\mathbf{r}) \simeq \frac{1}{2}\hat{q}(\xi)r^2\,, \tag{A.3}$$

where the path integral in (A.1) can be evaluated in a saddle point approxi-

mation. This approximation is known to lead to results which are physically equivalent [45] to other approaches. For a hard parton which transverses a time-independent medium of length L, we have $\hat{q}(\xi) = \hat{q}_0\,\Theta(L-\xi)$. For the realistic case of an expanding medium [10, 69, 70], the radiation spectrum is the same as that for an equivalent static medium of appropriately rescaled transport coefficient. This dynamical scaling law is used to define in (2.4) and (2.5) the only medium-dependent parameters ω_c and R. In Fig. A.1 the medium-modified part of the $\mathbf{k}_\perp$ integrated gluon energy distribution (A.1) is plotted for different values of m/E and $R = \omega_c L$ where $\omega_c = \frac{1}{2}\hat{q}\,L^2$.

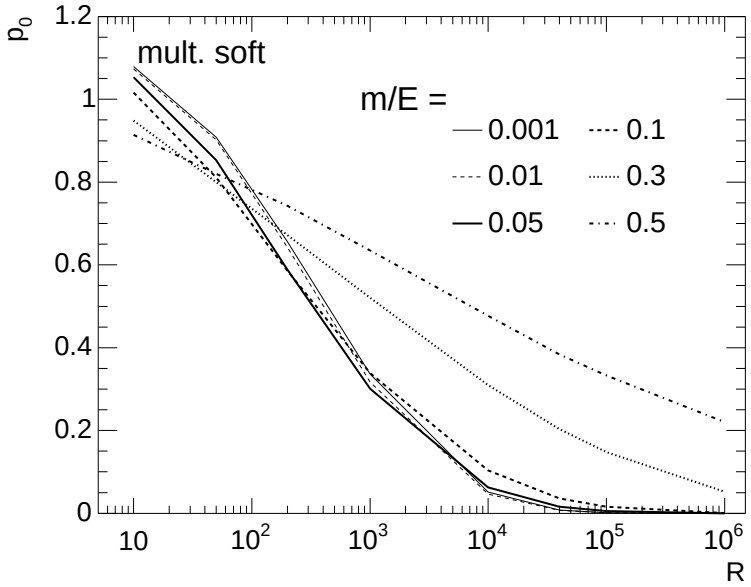

Fig. A.2. Discrete part p_0 of the quenching weight (A.4) as a function of R for different values of m/E.

The probability that in the parton fragmentation process of the hard massive quark, an additional amount ΔE of the initial quark energy is lost due to multiple medium-induced gluon radiation, can be modeled by a Poissonian process [34],

$$P(\Delta E/\omega_c, R, m/E) = \sum_{n=0}^{\infty} \frac{1}{n!}\left[\prod_{i=1}^{n}\int \mathrm{d}\omega_i \frac{dI^{\mathrm{med}}(\omega_i)}{d\omega}\right] \times\delta\left(\Delta E - \sum_{i=1}^{n}\omega_i\right)\exp\left[-\int \mathrm{d}\omega \frac{dI^{\mathrm{med}}}{d\omega}\right] . \tag{A.4}$$

We calculate this probability distribution via its Mellin transform as described in Ref. [34, 45]. It has a discrete and a continuous part

$$P(\Delta E/E, R, \omega_c) = p_0(R, m/E)\delta(\Delta E/\omega_c) + p(\Delta E/\omega_c, R, m/E)\,. \tag{A.5}$$

The discrete contribution p_0 is plotted in Fig. A.2. It denotes the probability that the hard parton escapes the collision region without further interaction [69]. Accordingly, this probability decreases with increasing density or increasing in-medium path length. For sufficiently large in-medium path length or density, $R = \omega_c\, L > 100$, the discrete part p_0 also increases with m/E —this is consistent with a mass-dependent reduction of parton energy loss.

The continuous part of (A.5) denotes the probability that the hard parton loses an additional energy ΔE due to medium-induced gluon radiation. As seen in Fig. A.3, this part increases with increasing in-medium path length or increasing density, since it depends on $\Delta E/(\hat{q}L^2/2) = \Delta E/\omega_c$. Also, for sufficiently large $R \gtrsim 1000$, the probability of losing a large energy ΔE is seen to decrease with increasing mass, as expected for a mass-dependent reduction of parton energy loss. In contrast, for the parameter range $R < 1000$, the relation between parton energy loss and mass dependence is more complicated and not monotonic, see Fig. A.3 for details. The latter case is of little practical relevance since it corresponds to very small medium effects, see also [45].

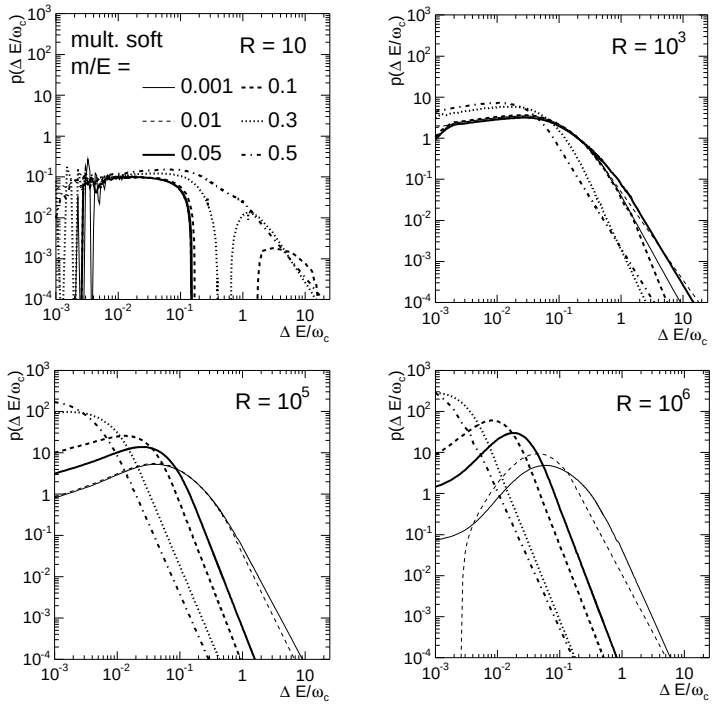

Fig. A.3. Continuous part of the quenching weight (A.4) for different values of R and of m/E.

The quenching weight $P(\Delta E/\omega_c, R, m/E)$ is a generalized probability which is normalized to unity. We have checked that the numerical results presented in Figs. A.2 and A.3 satisfy the normalization condition

$$\int_0^\infty \mathrm{d}(\Delta E/\omega_c) P(\Delta E/E, R, \omega_c)$$
$$= p_0(R, m/E) + \int_0^\infty \mathrm{d}(\Delta E/\omega_c) p(\Delta E/\omega_c, R, m/E) = 1\,. \qquad \text{(A.6)}$$

Our starting point, the gluon energy distribution (A.1), is derived in the eikonal limit and holds to leading order in $1/E$. In this high energy approximation, it is possible that for a finite parton energy E, the quenching weight has support in the region $\Delta E > E$. This is clearly an artifact of the formalism. We correct it by assuming that a parton which is predicted to lose more than its total energy has lost all its energy in the medium. To this end, we truncate $P(\Delta E/E)$ at $\Delta E = E$ but we ensure the normalization (A.6) by adding a δ-function [8, 9]

$$P_{\mathrm{nrw}}(\Delta E/E, R, \omega_c) = P(\Delta E/E, R, \omega_c)\,\Theta(1 - \Delta E/E)$$
$$+\delta(\Delta E/E - 1) \int_1^\infty \mathrm{d}\epsilon\, P(\epsilon)\,. \qquad \text{(A.7)}$$

The corresponding Monte Carlo implementation is: sample an energy loss ΔE and set the new parton energy to 0 if $\Delta E \geq E$.

The size of the remainder term $\int_1^\infty \mathrm{d}\epsilon\, P(\epsilon)$ has been used [8, 9] to estimate the systematic theoretical uncertainties in this formalism. These uncertainties increase with increasing parton energy loss and they decrease with increasing transverse momentum. For the nuclear modification factors R_{AA} of both light-flavored and heavy-flavored hadrons, they amount to typical uncertainties of ± 0.1 at $p_T = 5$ GeV and ± 0.05 at $p_T > 10$ GeV.

---

1. M. Gyulassy and X. N. Wang, Nucl. Phys. B **420** (1994) 583.
2. R. Baier, Y. L. Dokshitzer, A. H. Mueller, S. Peigne and D. Schiff, Nucl. Phys. B **484** (1997) 265.
3. B. G. Zakharov, JETP Lett. **65** (1997) 615.
4. U. A. Wiedemann, Nucl. Phys. B **588** (2000) 303.
5. M. Gyulassy, P. Levai and I. Vitev, Nucl. Phys. B **594** (2001) 371.
6. X. N. Wang and X. F. Guo, Nucl. Phys. A **696** (2001) 788.
7. X. N. Wang, Phys. Lett. B **579** (2004) 299.
8. A. Dainese, C. Loizides and G. Paic, Eur. Phys. J. C **38** (2005) 461.
9. K. J. Eskola, H. Honkanen, C. A. Salgado and U. A. Wiedemann, Nucl. Phys. A **747** (2005) 511.
10. M. Gyulassy, I. Vitev and X. N. Wang, Phys. Rev. Lett. **86** (2001) 2537.
11. A. Drees, H. Feng and J. Jia, arXiv:nucl-th/0310044.
12. I. Vitev and M. Gyulassy, Phys. Rev. Lett. **89** (2002) 252301.

13. T. Hirano and Y. Nara, Phys. Rev. C **66** (2002) 041901.
14. K. Adcox *et al.* [PHENIX Collaboration], Phys. Rev. Lett. **88** (2002) 022301.
15. S. S. Adler *et al.* [PHENIX Collaboration], Phys. Rev. C **69** (2004) 034910.
16. C. Adler *et al.* [STAR Collaboration], Phys. Rev. Lett. **89** (2002) 202301.
17. J. Adams *et al.* [STAR Collaboration], Phys. Rev. Lett. **91** (2003) 172302.
18. B. B. Back *et al.* [PHOBOS Collaboration], Phys. Lett. B **578** (2004) 297.
19. I. Arsene *et al.* [BRAHMS Collaboration], Phys. Rev. Lett. **91** (2003) 072305.
20. C. Adler *et al.* [STAR Collaboration], Phys. Rev. Lett. **90** (2003) 082302.
21. J. Adams *et al.* [STAR Collaboration], Phys. Rev. Lett. **93** (2004) 252301.
22. U. A. Wiedemann, J. Phys. G **30** (2004) S649.
23. A. Majumder and X. N. Wang, Phys. Rev. D **70** (2004) 014007.
24. A. Majumder and X. N. Wang, arXiv:hep-ph/0411174.
25. A. Majumder, E. Wang and X. N. Wang, arXiv:nucl-th/0412061.
26. C. A. Salgado and U. A. Wiedemann, Phys. Rev. Lett. **93** (2004) 042301.
27. S. Pal and S. Pratt, Phys. Lett. B **574** (2003) 21.
28. N. Armesto, C. A. Salgado and U. A. Wiedemann, Phys. Rev. Lett. **93** (2004) 242301.
29. N. Armesto, C. A. Salgado and U. A. Wiedemann, arXiv:hep-ph/0411341.
30. Y. L. Dokshitzer and D. E. Kharzeev, Phys. Lett. B **519** (2001) 199.
31. N. Armesto, C. A. Salgado and U. A. Wiedemann, Phys. Rev. D **69** (2004) 114003.
32. B. W. Zhang, E. Wang and X. N. Wang, Phys. Rev. Lett. **93** (2004) 072301.
33. M. Djordjevic and M. Gyulassy, Nucl. Phys. A **733** (2004) 265.
34. R. Baier, Y. L. Dokshitzer, A. H. Mueller and D. Schiff, JHEP **0109** (2001) 033.
35. A. Dainese, Eur. Phys. J. C **33** (2004) 495.
36. T. Sjostrand, L. Lonnblad and S. Mrenna, arXiv:hep-ph/0108264.
37. H. L. Lai *et al.* [CTEQ Collaboration], Eur. Phys. J. C **12** (2000) 375.
38. K. J. Eskola, V. J. Kolhinen and C. A. Salgado, Eur. Phys. J. C **9** (1999) 61.
39. A. Tai [STAR Collaboration], J. Phys. G **30** (2004) S809.
40. J. Adams *et al.* [STAR Collaboration], arXiv:nucl-ex/0407006.
41. S. Batsouli, S. Kelly, M. Gyulassy and J. L. Nagle, Phys. Lett. B **557** (2003) 26.
42. X. Y. Lin, arXiv:hep-ph/0412124.
43. N. Carrer and A. Dainese, arXiv:hep-ph/0311225.
44. M. L. Mangano, P. Nason and G. Ridolfi, Nucl. Phys. B **373** (1992) 295.
45. C. A. Salgado and U. A. Wiedemann, Phys. Rev. D **68** (2003) 014008.
46. The FORTRAN subroutine for quenching weights of massive quarks can be downloaded from http://www.pd.infn.it/∼dainesea/qwmassive.html.
47. C. W. De Jager, H. De Vries and C. De Vries, Atom. Data Nucl. Data Tabl. **14** (1974) 479.
48. Z. W. Lin, R. Vogt and X. N. Wang, Phys. Rev. C **57** (1998) 899.
49. M. I. Gorenstein, A. P. Kostyuk, H. Stocker and W. Greiner, Phys. Lett. B **509** (2001) 277.
50. A. Andronic, P. Braun-Munzinger, K. Redlich and J. Stachel, Phys. Lett. B **571** (2003) 36.
51. Z. W. Lin and D. Molnar, Phys. Rev. C **68** (2003) 044901.

52. H. van Hees and R. Rapp, arXiv:nucl-th/0412015.
53. G. D. Moore and D. Teaney, arXiv:hep-ph/0412346.
54. P. Romatschke and M. Strickland, arXiv:hep-ph/0408275.
55. M. G. Mustafa, arXiv:hep-ph/0412402.
56. J. Adams *et al.* [STAR Collaboration], Phys. Rev. Lett. **92** (2004) 052302.
57. S. S. Adler *et al.* [PHENIX Collaboration], Phys. Rev. Lett. **91** (2003) 172301.
58. S. S. Adler *et al.* [PHENIX Collaboration], arXiv:nucl-ex/0409028.
59. K. J. Eskola, K. Kajantie, P. V. Ruuskanen and K. Tuominen, Nucl. Phys. B **570** (2000) 379.
60. N. Armesto, C. A. Salgado and U. A. Wiedemann, Phys. Rev. Lett. **94** (2005) 022002.
61. A. Accardi *et al.*, arXiv:hep-ph/0310274.
62. I. P. Lokhtin, L. I. Sarycheva, A. M. Snigirev and K. Y. Teplov, Eur. Phys. J. C **37** (2004) 465.
63. B. W. Zhang, E. K. Wang and X. N. Wang, arXiv:hep-ph/0412060.
64. M. Djordjevic, M. Gyulassy and S. Wicks, arXiv:hep-ph/0410372.
65. W. C. Xiang, Y. X. Mao, J. Liu, H. T. Ding, D. C. Zhou and D. Rohrich, arXiv:hep-ph/0501041.
66. R. Thomas, B. Kampfer and G. Soff, arXiv:hep-ph/0405189.
67. Q. Wang and X. N. Wang, arXiv:nucl-th/0410049.
68. X. N. Wang, Phys. Rev. C **58** (1998) 2321.
69. C. A. Salgado and U. A. Wiedemann, Phys. Rev. Lett. **89** (2002) 092303.
70. R. Baier, Y. L. Dokshitzer, A. H. Mueller and D. Schiff, Phys. Rev. C **58** (1998) 1706.